Easy-understudying simulator for an extraction process of natural matrixes with supercritical CO_2 in a packed bed column.

*A.Cabeza[a], F. Sobrón[a]., J. García-Serna[a]. M. J. Cocero[a]**

[a]High Pressure Processes Group, Department of Chemical Engineering and Environmental Tech., University of Valladolid, 47011 Valladolid, Spain

**Corresponding author: mjcocero@iq.uva.es*

Abstract

The aim of this work was to develop a user-friendly Excel interface to adjust the yields of an extraction column. Moreover, this program could simulate the dynamic concentration profiles inside the column, being a useful teaching tool. The model comprises non-stationary mass balances for the recovered compounds in both phases (solid and supercritical CO_2). The model was tested by reproducing the extraction of two samples: sesame seeds and coffee beans (average deviations of 7.41% and 10.35%, respectively). These samples were selected to demonstrate the feasibility of reproducing processes whose mass transfer limitation is different. Thus, for the sesame seeds, the extraction process was controlled by both the external mass transfer and oil solubility, since the seeds were grinded. On the contrary, for coffee grains, the internal diffusion controls the extraction as the whole grain is required. Regarding solubility, a Henry's linear relation between solid and CO_2 concentration was assumed.

Keywords: Supercritical CO_2, Excel interface, oil extraction, decaffeination, modelling, natural matrixes.

1. Introduction

Extraction of oil or other compounds from natural solid matrixes is a well-known process in industry. For decades, it has been successfully performed by organic solvents, generating an exhausted solid, which presents a residual amount of solvent, and a liquid rich in the extracted compound. This solid generally requires a purification to remove this organic residue (due to healthy or quality considerations) and the obtained liquid could also need another stage to recover the extracted substance. Therefore, the conventional solid-liquid extraction process always needs two stages: the extraction with the solvent and a purification with another material agent or energy. For this reason, other solvents has been considered, being supercritical fluids (SCF) the most extended option. Supercritical fluid extraction (SFE) would have two main advantages against the conventional method. The first would be that solubility in the SCF is totally controlled by pressure and temperature. So, the recovered compounds can be completely separated from the solvent only with a change in these variables. The second would be that as the solvent is a SCF, only with a depressurization the exhausted solid would be clean of residual solvent. The most common SCF for these extractions is CO_2 because its critical point is relative low (7.38 MPa and 31.1 ºC) and because it is non-toxic and non-flammable [1-3].

This extraction of certain compounds from natural raw material with supercritical CO_2 ($ScCO_2$) has been thoroughly studied and several articles can be found in literature [4-7]. *Sara Spinelli et al.* [4] studied the SFE with CO_2 and ethanol as entrainer of phenolic compounds and flavonoids from brewer's spent grain (BSG). They analysed the effect of temperature, pressure and entrainer concentration, obtaining that $ScCO_2$ with a 60% of ethanol archives yields of 0.35 mg/g BSG and 0.22 mg/g BSG for phenolic compounds and flavonoids, respectively. *Amit Rai et al.* [5] assessed the oil extraction from sunflower seeds varying temperature, pressure, particle diameter, flow rate and co-solvent or entrainer concentration (ethanol). Their result was that this extraction reach a yield of 54.37 wt% with a 5% of co-solvent. *Hazuki Nerome et al.* [6] performed a work about the extraction of pigments from Saffron (*Crocus sativus L.*) with $ScCO_2$ and two co-solvents (water and methanol) obtaining higher yields than in the conventional process. Thus, $ScCO_2$ has been used successfully to perform extraction of herbs, seeds and grains and with high yields. Moreover, some SFE, such as coffee beans or green-tea decaffeination are already at industrial scale [8].

Regarding its modelling, there are also a lot of works about it [7, 9, 10]. It is worth highlighting the work of *H. Sovová* [9] who developed a model for $ScCO_2$ extraction with 3 different solutions, depending on the mass transfer limitation. In the same way, *Onur Döker et al.* [10] studied the modelling of the SFE of oil from sesame seeds with $ScCO_2$. They compared two options: Shrinking core model and Broken and intact cell model, obtaining that the first would be the best option to reproduce the extraction (deviations lower than 8.54% and 14.65% respectively). Similarly, *B. Honarvar et al.* [11] also assessed the modelling for the extraction of sesame seeds but comparing three different equilibrium relations: Henry's, Freundlich's and Brunauer, Emmet and Teller's. Their result was that the latter would be the most appropriate to reproduce the experimental yields (deviations of 9.84 %, 7.42% and 5.28% respectively). However, all these previous studies are focused in the reproduction of the experimental data without further considerations. Therefore, they do not include the simulation of the extracted compound in both phases, which would be a key factor in order to understand how extraction is and how the operational variables affect it.

Thus, the aim of this work is to develop a user-friendly Excel interface to adjust the extraction yields and to simulate the dynamic concentration profiles inside the extraction column. This interface would be based on a model for SCE which would be validated for two of the most studied extraction process, e. g. oil extraction from seeds (sesame seeds) and coffee beans decaffeination. Moreover, this Excel program could be used to simulate the effect of particle dimeter, volumetric flow, pressure and temperature in the extraction.

2. Extraction process and available data

2.1. Extraction process

A typical configuration for a SFE process is shown in Figure 1. It consist of a gas bottle (T-01), a heat exchanger (H-01), a pump (P-01), the extraction column (E-01) and an expansion valve (V-01) and vessel (T-02).

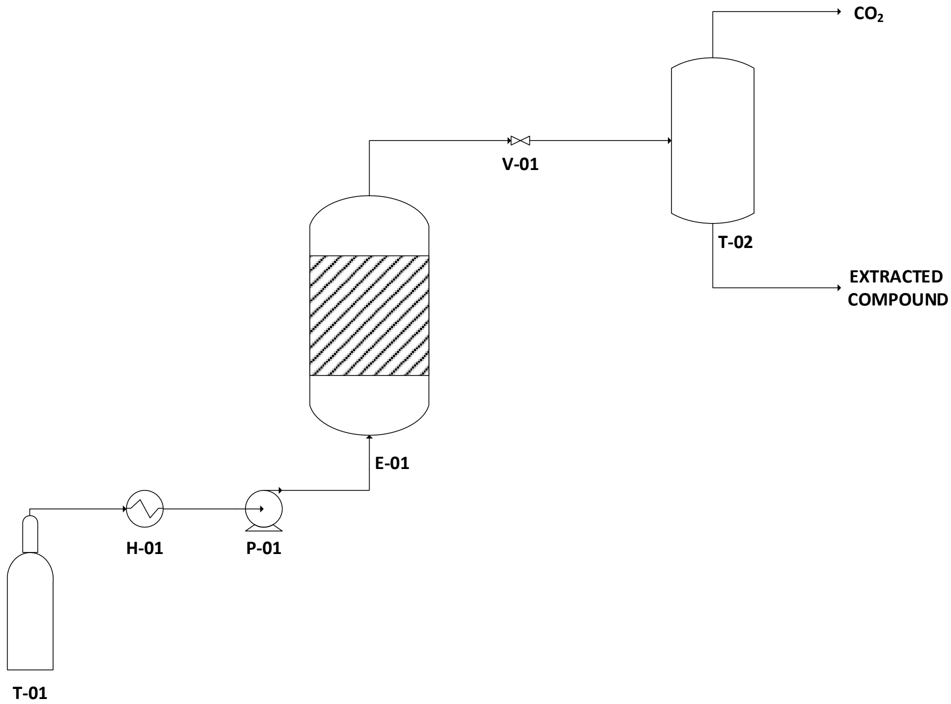

Figure 1: Process flow diagram of a typical SFE process with CO_2. T-01: gas bottle, H-01: heat exchanger, P-01: pump, E-01: extraction column, V-01: expansion valve and T-02: expansion vessel.

The operation starts with the conditioning of the stream from the bottle T-01 in the heat exchanger H-01 and in the pump P-01. This stage is done in order to transform the gas into a SCF at the desired operational conditions. Once this stream is already a SCF, it is fed to the extraction column E-01 to separate the desired compound from the solid matrix. Therefore, the output stream of the column E-01 is composed by the SCF and the desired compound. Finally, it is expanded in the valve V-01 to separate the extracted compound from the solvent in T-02 by the transformation of the SCF into a gas due to this pressure change.

2.2. Available data and raw materials

As it as mentioned in section 1, the raw materials assessed in this work are sesame seeds and coffee grains, which were selected for two reason. The first is that they are examples of the most studied SFE process: oil recovering and decaffeination. On the other hand, the second is related with mass transfer limitations. Generally, in an oil extraction seeds are previously milled whereas, in a coffee grain decaffeination, grains are not physically pre-treated. Therefore, in the former several stages with a different mass transfer control are expected (Figure 2-b) and the effect of temperature, pressure, volumetric flow and particle diameter can be considered. On the contrary, in coffee grains only one stage is awaited and particle diameter can not be taken into account since they are not milled.

The data from the oil extraction from sesame seeds were taken from *Onur Döker et al.* [10], who treated samples of 4 g (56 % of oil) with $ScCO_2$. For caffeine extraction, the data were found in *Hulya Peker et al.* [12], who worked with 0.86 g of coffee with a content of 3.8% of caffeine and humidified $ScCO_2$.

The whole set of experiments and their operational conditions are listed in Table 1.

Table 1: Studied experiments and their operational conditions.

Experiment	Raw material	T[1] ºC	P[2] bar	dp[3] µm	Q[4] ml/min
1	Sesame seeds	50	350	450	2.00
2	Sesame seeds	50	300	450	2.00
3	Sesame seeds	50	250	450	2.00
4	Sesame seeds	50	350	450	2.00
5	Sesame seeds	50	350	890	2.00
6	Sesame seeds	50	350	1180	2.00
7	Sesame seeds	50	350	450	1.00
8	Sesame seeds	50	350	450	2.00
9	Sesame seeds	50	350	450	3.00
10	Sesame seeds	60	350	450	2.00
11	Sesame seeds	60	300	450	2.00
12	Sesame seeds	60	250	450	2.00
13	Sesame seeds	70	350	450	2.00
14	Sesame seeds	70	300	450	2.00
15	Sesame seeds	70	250	450	2.00
16	Coffee grains	40	138	*	1.51
17	Coffee grains	50	103	*	1.51
18	Coffee grains	50	138	*	1.51
19	Coffee grains	50	193	*	1.51
20	Coffee grains	50	138	*	0.68
21	Coffee grains	50	138	*	1.51
22	Coffee grains	50	138	*	4.59
23	Coffee grains	64	138	*	1.51
24	Coffee grains	80	138	*	1.51

[1]Operating temperature. [2] Operating pressure. [3] Average particle diameter. [4] Operating flow. * Variable not considered in this experiment.

3. Extraction theory

3.1. Mass transfer during a extraction from a solid raw material

In Figure 2-a all the steps involved in an extraction process are shown. First, the desired compound should be solved by the SCF (step 1). Then, it diffuses (step 2) in the pores of the raw material up to reach the solid external surface. Finally, it should go through the boundary layer (step 3) of the SCF in order to be extracted from the solid. The relative value between these steps affect strongly to the extraction, as can be seen in Figure 2-b.

In Figure 2-b an extraction curve (yield vs time) with three different stages (A, B and C) is showed. Stage A corresponds to a fast extraction process, which means an extraction with no internal diffusion effect (step 2 in Figure 2-a). This stage can take place if the material has been previously milled or if the extraction is performed in the external surface of the solid. On the other hand, stage B is related with a process in which the external transport and the internal diffusion have similar values or with low solubility. The former can occur when low internal diffusion exits, therefore when the compound solves near the external solid surface. Finally, stage C takes place when internal diffusion controls the extraction, which means that the solubilisation is done far from the external solid surface.

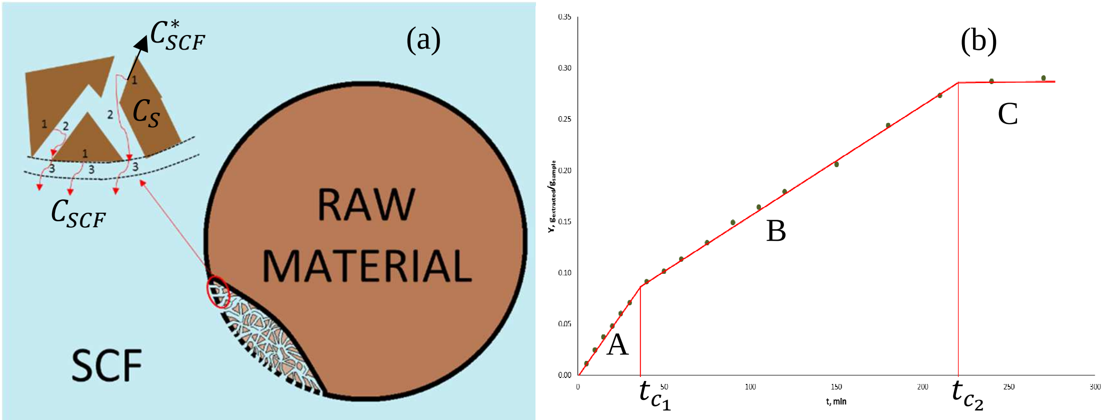

Figure 2: Mass transfer steps during an extraction (a) and their effect in the extraction curve (b). 1: solubilisation, 2: internal diffusion of the extracted compound and 3: external mass transfer of the extracted compound. A: extraction controlled by the external transport, B: extraction controlled by both: external transport and internal diffusion and C: extraction controlled by internal diffusion.

3.2. Solubility in SCF

SCFs have transport properties between liquids and gases, such as densities similar to liquids and diffusivities closer to gases [1, 2]. Moreover, changes in the dielectrical properties are also observed when pressure and temperature are increased [13]. On the other hand, temperature and pressure also affect density, which enhances solving properties [2]. Therefore, it is confirmed that solubility in SCFs is totally controlled by temperature and pressure (as it was mentioned in section 1)

3.2.1. Co-solvents

Although solubility in SCF is easily controllable, it also has some restrictions. For instance, $ScCO_2$ has a low polarity [6, 14], which means that its efficiency to extract polar compounds is low. Therefore, in order to increase its solvent capacity a small amount of a polar substance (co-solvent) is added to the SCF. Some typical examples of co-solvents are: ethanol, methanol and water.

3.2.2. Solubility calculations

Solubility in $ScCO_2$ can be obtained from the equilibrium condition of equal fugacities in both phases for each compound and using equations of states [15]. However, these type of thermodynamic calculations in the simulator would make the model more difficult, increasing the calculating times and reducing the appealing of the developed program. Therefore, a direct fitting solubility was used in this work, similarly as it was done in previous studies [10, 11].

3.3. Model

The model of the process was done applying a non-stationary mass balance for the recovered compound in both phases. In order to simplify the modelling it was assumed that (1) the bed porosity remains constant, that (2) there are no diffusional transport along the length of the column and that (3) the solubilisation follows a Henry's relation. The balance for the SCF is shown in Eq. (1) and for the solid in Eq. (2).

$$\frac{\delta C_{SCF}}{\delta t} = \frac{1}{\mathcal{E}} \cdot \left[-\frac{u}{L} \cdot \frac{\delta C_{SCF}}{\delta z} + K \cdot a \cdot (C^*_{SCF} - C_{SCF}) \right] \qquad (1)$$

$$\frac{dC_s}{dt} = \frac{1}{1-\mathcal{E}} \cdot [-K \cdot a \cdot (C^*_{SCF} - C_{SCF})] \qquad (2)$$

Where C^*_{SCF} corresponds to the equilibrium concentration of the extracted compound in the SCF calculated by a Henry's relation with the concentration in the solid (C_s): $C^*_{SCF} = H \cdot C_s$.

Regarding the mass transfer between both phases, a global coefficient from the equilibrium concentration and the concentration in the SCF phase was used. In order to include the three possible stages defined in section 3.1, it was defined as a function of the times (Eq. (3)) when the change between these stages takes places (Figure 2-b).

$$K \cdot a = \frac{k_{SCF} \cdot a_{SCF} \cdot \left(\frac{F}{1 + e^{-(t - t_{c_1})}} \right)}{1 + e^{(t - t_{c_2})}} + \frac{k_s \cdot a_s}{1 + e^{-(t - t_{c_2})}} \qquad (3)$$

Where F is a correction factor in order to include the stage B.

These times of change between stages would be the breaking times and they would be a reverse function of the mass easy to extract. Thus, t_{c1} would be a function of that mass whose extraction would be controlled by a short internal diffusion and external mas transport. And t_{c2} would be related with an extraction dominated by external transport.

3.3.1. Resolution

The model formed by Eq. (1) and (2) constitutes a set of partial differential equation. This set was discretised by the orthogonal collocation on finite elements method, obtaining a set of ordinary differential equation. The latter was solved by the Runge-Kutta's method with 8th order of convergence [16].

On the other hand, the optimization problem related with the adjustment of the experimental extraction curves was solved by two methods. The first was the Simplex-Nelder-Mead's method to obtain an initial solution of the problem. Finally, this solution was re-optimized applying the Broyden–Fletcher–Goldfarb–Shanno's method. The objective function was the Absolute Average Deviation (A.A.D.) between the simulated and experimental yields (Eq. (4)).

$$A.A.D. = \sum_{i=1}^{n} \frac{1}{n} \cdot \frac{\left| x_{i_{EXP}} - x_{i_{SIM}} \right|}{x_{i_{EXP}}} \cdot 100 \qquad (4)$$

4. Results and discussion

4.1. Pressure and temperature effect: solubility changes

From Figure 3 the effect of temperature and pressure can be observed. Figure 3.a - b show the evolution of the extraction yield for oil from sesame seeds and caffeine from coffee beans, respectively. It can be observed that, for both processes, the yield increases with pressure. This behaviour agrees with the discussion in section 3.2 since density rises with pressure (from 834 kg/m^3 at 50 ºC and 250 bar up to 899 kg/m^3 at 50 ºC and 350 bar). So, solubility also should grow with pressure.

On the other hand, in Figure 3.b-c the role of temperature in oil extraction and coffee beans decaffeination is shown, respectively. For oil extraction, a decrement in the yield can be observed due to the reduction of density (and solubility) with temperature (from 834 kg/m^3 at 50 ºC and 250 bar up to 737 kg/m^3 at 70 ºC and 250 bar). Behaviour that also agrees with section 3.2. Moreover, it is remarkable that at 250 bar and 70 ºC the stage B appears because of the low solubility (see section 3.1). However, for the decaffeination an increment in the yield was observed, although density decreased with temperature. This deviation from the expected evolution can be explained by the co-solvent [12]. As the operation is performed by a mixture of $ScCO_2$ and water, there will be a partition coefficient of caffeine between the two phases. This coefficient is defined as the ratio of the caffeine concentration in the SCF and its equilibrium concentration in water, which has been found that increases with temperature at high pressures.

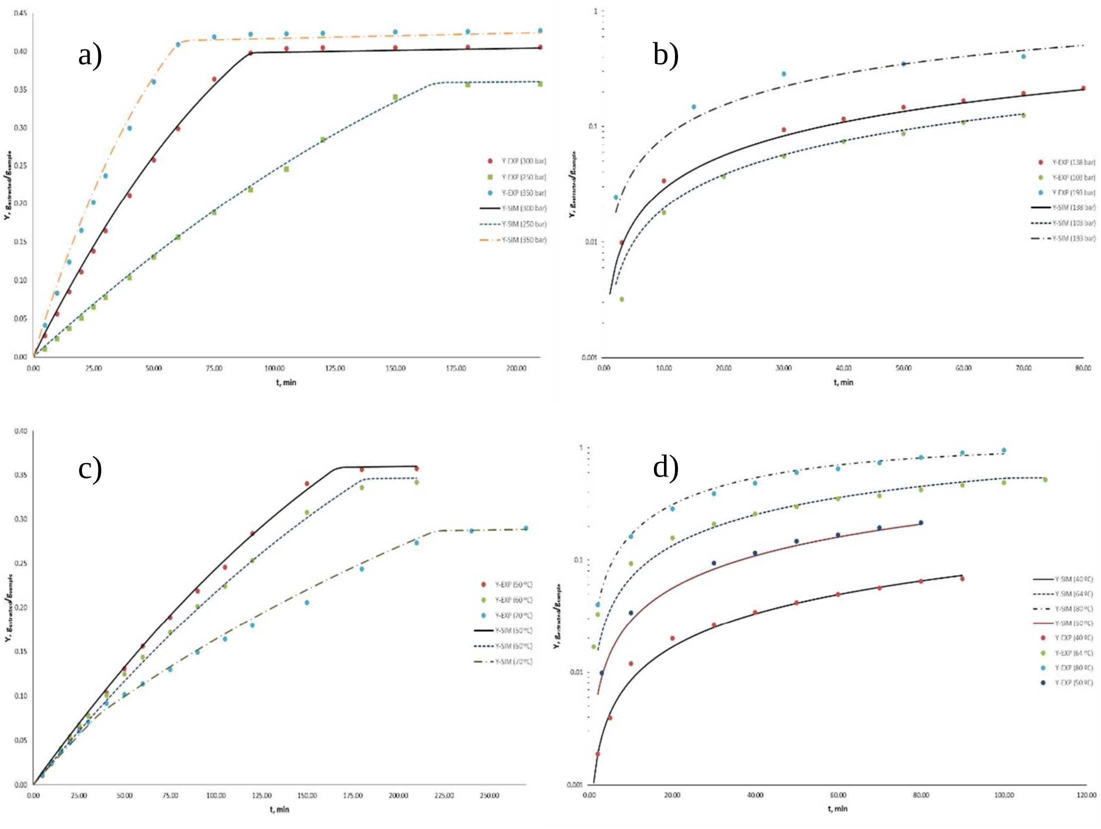

Figure 3: Effect of the operating temperature and pressure in a SCF extraction. (a) Effect of the operating pressure in the oil extraction from sesame seeds at 50 ºC, 2 mL/min and 450 μm. (b) Effect of the operating pressure in the caffeine extraction from coffee beans at 50 ºC and 1.51 mL/min. (c) Effect of the operating temperature in the oil extraction from sesame seeds at 250 bar, 2 mL/min and 450 μm. (d) Effect of the operating temperature in the caffeine extraction from coffee beans at 138 bar and 1.51 mL/min. Y-SIM: simulated extraction yield ($g_{extracted}/g_{sample}$). Y-EXP: experimental extraction yield ($g_{extracted}/g_{sample}$).

4.2. Particle diameter and flow effect: mass transfer changes

In Figure 4.a-b the variation in the extraction yield with the volumetric flow is shown for a caffeine and oil extraction process, respectively. In both cases, the yield increases with flow since mass transfer is enhanced. However, there is a significant difference between them. In the oil extraction, all the curves tends to a similar value of yield, which means that the improvement in mass transfer only makes faster the process. While in decaffeination the yield is also increased. This discrepancy would be related with the fact that in oil extraction the seeds has been previously milled and a certain amount of oil is free to be recovered. In contrast, in decaffeination the extraction is performed to the whole grain and there is a real mass transfer limitation in the boundary layer (see section 3.1). Regarding the particle diameter, its effect in the oil recovering is shown in Figure 4.c, where it can be checked that the lower de particle diameter is, the greater extraction is obtained. This dependence is related with its effect in the external and internal mass transfer. So, a low diameter means more exchange surface, which enhances the external mass transfer, and less way to diffuse inside the solid.

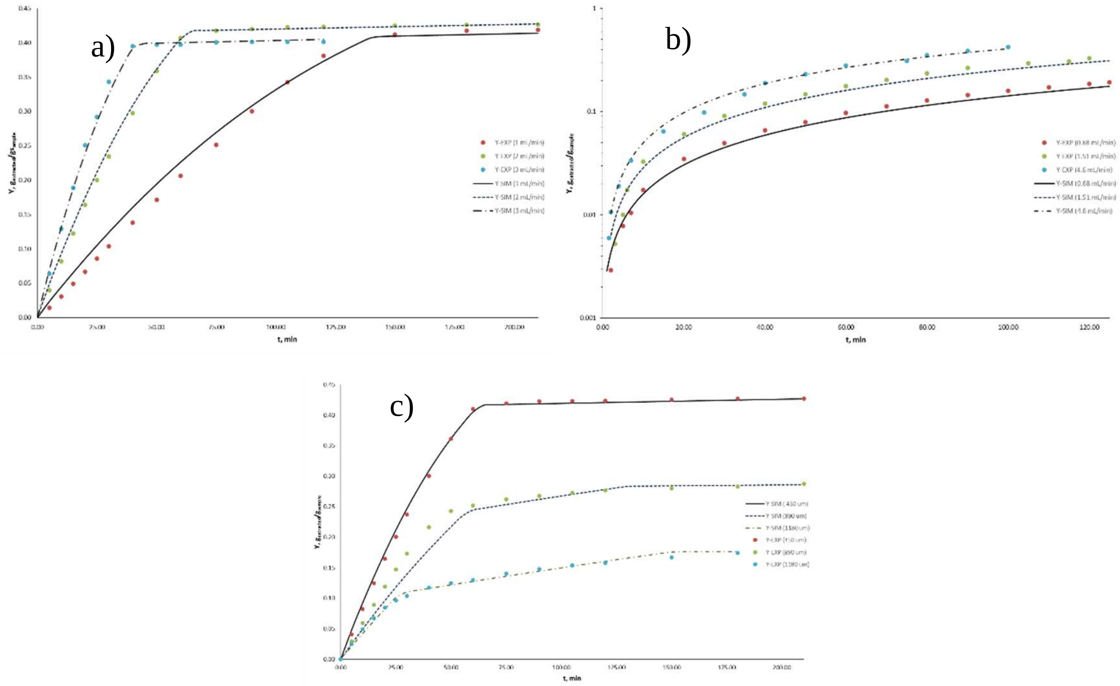

Figure 4: Particle diameter and volumetric flow effects. (a) Role of the volumetric flow in the oil extraction from sesame seeds at 50 ºC, 350 bar and 450 µm. (b) Role of the volumetric flow in the oil caffeine from coffee beans at 50 ºC and 138 bar. (c) Role of the particle diameter in the oil extraction from sesame seeds at 50 ºC, 350 bar and 2 mL/min. Y-SIM: simulated extraction yield ($g_{extracted}/g_{sample}$). Y-EXP: experimental extraction yield ($g_{extracted}/g_{sample}$).

4.3. Fittings

In Figure 3 and Figure 4 the simulated behaviour with the model is shown and the A.A.D. of all the adjustments is arrayed in Table 2. In this table, it can be seen that the average deviation for sesame oil extraction and decaffeination were 7.41% and 10.35%, respectively. The fact that the deviation was greater in decaffeination was expected since it was performed with a co-solvent and its effect was not taken into account separately in the model. All in all, all de deviations are relatively low and it can be checked that the simulation agrees with the experimental data. So, it can be concluded that the approach developed in section 3.3 can reproduce the experimental yields, including the effect of all the operational variables. The fitted parameters as long as their regression coefficients are listed from Table 3 to Table 7.

Table 2: A.A.D. of the adjustments.

Experiment	A.A.D. %
1	6.89
2	3.62
3	8.90
4	6.62
5	10.54
6	4.49
7	16.94
8	6.32
9	6.29
10	7.14
11	3.48
12	4.95
13	9.49
14	8.93
15	6.68
16	7.82
17	6.75
18	7.75
19	18.89
20	10.09
21	14.61
22	6.68
23	15.17
24	5.38
Average Seeds	7.41
Average Beans	10.35

4.3.1. Equilibrium constant

In Table 3 and Figure 5.a the calculated values of the equilibrium constant and its regression coefficient for sesame oil are shown. In the same way, in Table 4 and Figure 6.a for caffeine. For sesame oil, it can be checked that its behaviour agrees with the theory showed in section 3.2. So, an increment in temperature generated a lineal decrement in density (Figure 5.b) and a lineal diminution of the solubility. However, for caffeine there is a discrepancy. In Figure 6.b it can be seen that density decreases logarithmically with temperature but the solubility grows exponentially (Figure 6.a). In parallel, solubility is also increased exponentially with pressure (Figure 6.c) though density tends to a maximum (Figure 6.d). This deviation could be related again with the fact that water is used as a co-solvent and, at the operating conditions, and increment in temperature and pressure would enhance the solubility and the extraction (section 4.1).

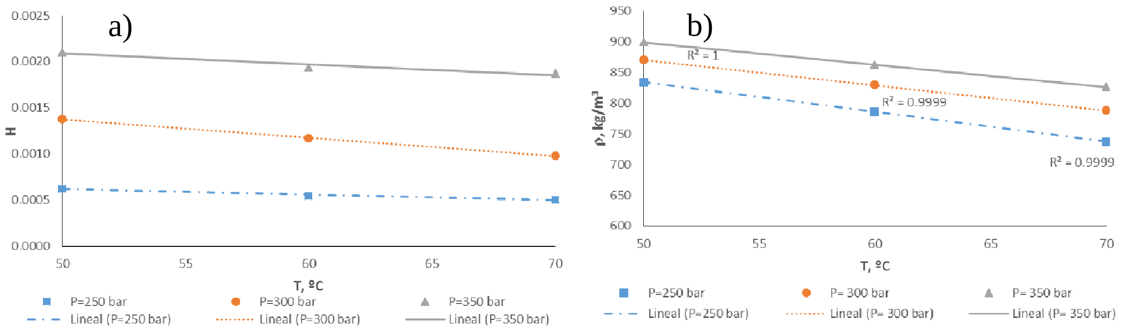

Figure 5: Sesame oil equilibrium constant evolution with temperature and pressure (a) and changes in $ScCO_2$ with temperature and pressure.

Table 3: Fitted sesame oil equilibrium constant.

H (dimensionless)			
T(ºC)	P(bar)		
	250	300	350
50	6.24E-04	1.38E-03	2.11E-03
60	5.45E-04	1.17E-03	1.94E-03
70	5.07E-04	9.84E-04	1.87E-03
R^2	0.96	0.999	0.94

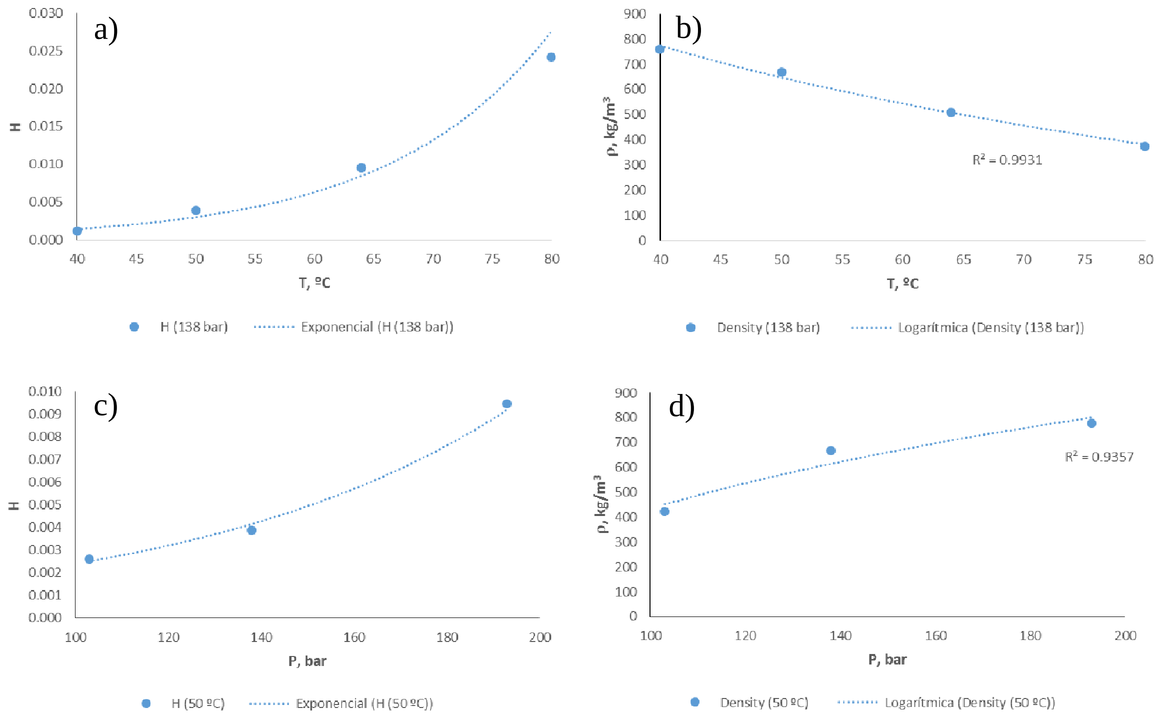

Figure 6: Caffeine equilibrium constant evolution with temperature (a) and pressure (c) and changes in $ScCO_2$ density with temperature (b) and pressure (d).

Table 4: Fitted caffeine equilibrium constant.

H (dimensionless)

T(ºC)		P(bar)	
40	1.14E-03	103	2.62E-03
50	3.87E-03	138	3.87E-03
64	9.56E-03	193	9.44E-03
80	2.41E-02		
R^2	0.97		0.991

4.3.2. Mass transfer coefficient

The external and internal mass transfer coefficients for sesame oil are showed in Figure 7 and Table 5. The obtained evolution with the flow and particle diameter was the expected result for both coefficients. Therefore, the external coefficients grows with the former and decreases with the latter. Regarding the internal coefficients, it was independent from the flow and it decreases with particle diameter. In addition, the correction factor for stage B (F) is also listed in Table 5. Its behaviour was also the awaited result, decreasing with pressure and particle diameter.

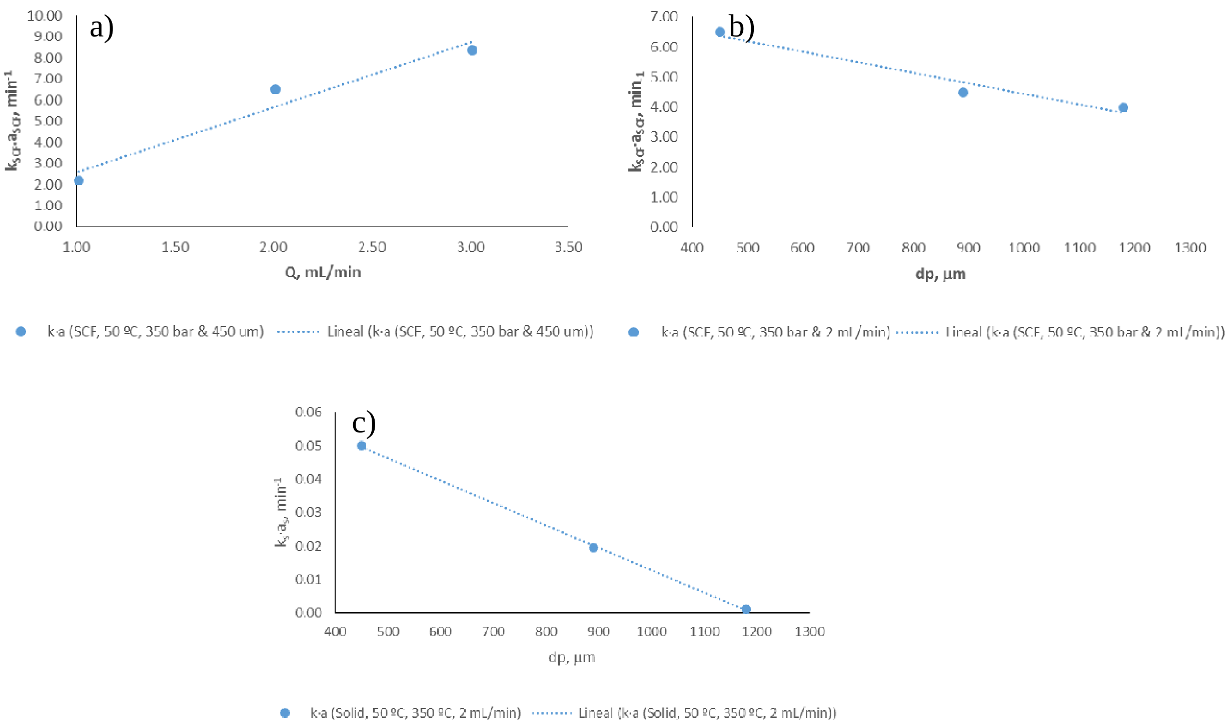

Figure 7: Sesame oil external mass transfer dependency with flow (a) and particle diameter (b) and internal mass transfer evolution with particle diameter (c).

Table 5: Fitted sesame oil external and internal mass transfer coefficients, including the correction factor (F) for stage B.

$k_s \cdot a_s$ (min^{-1})		$k_{SCF} \cdot a_{SCF}$ (min^{-1})	
d_p(µm)		dp(µm)	
450	5.00E-02	450	6.5
890	1.95E-02	890	4.5
1180	1.00E-03	1180	4.0

R^2	0.95		0.95
$k_{SCF}\cdot a_{SCF}$ (min^{-1})			
Q(mL/min)			
1		2.18	
2		6.50	
3		8.36	
R^2		0.9995	
F (dimensionless)			
P(bar)		dp(µm)	
300	0.68	590	0.08
250	0.32	1180	0.07

On the other hand, for caffeine the global mass transfer coefficient was calculated (Table 6 and Figure 8) because during its extraction only the stage B was observed. So, the fact that its evolution with flow tends to a maximum would be correct since flow only enhances the external mass transfer.

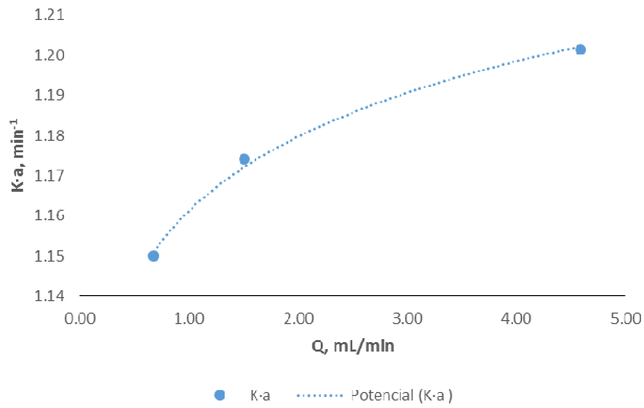

Figure 8: Caffeine global mass transfer coefficient dependency with flow.

Table 6: Fitted global mass transfer coefficient for caffeine.

K·a (min^{-1})	
Q (mL/min)	
0.68	1.15
1.51	1.17
4.59	1.20
R^2	0.995

4.3.3. Breaking times

The calculated values for the braking times (t_{c1} and t_{c2}) are shown in Figure 9 and Table 7. As it was mentioned in section 3.1, the parameters would be a reverse function of mass able to be extracted. Therefore, they should decrease with pressure and flow and increase with temperature and particle diameter, tending to a minimum and maximum value, respectively. Being this behaviour the obtained during the optimization.

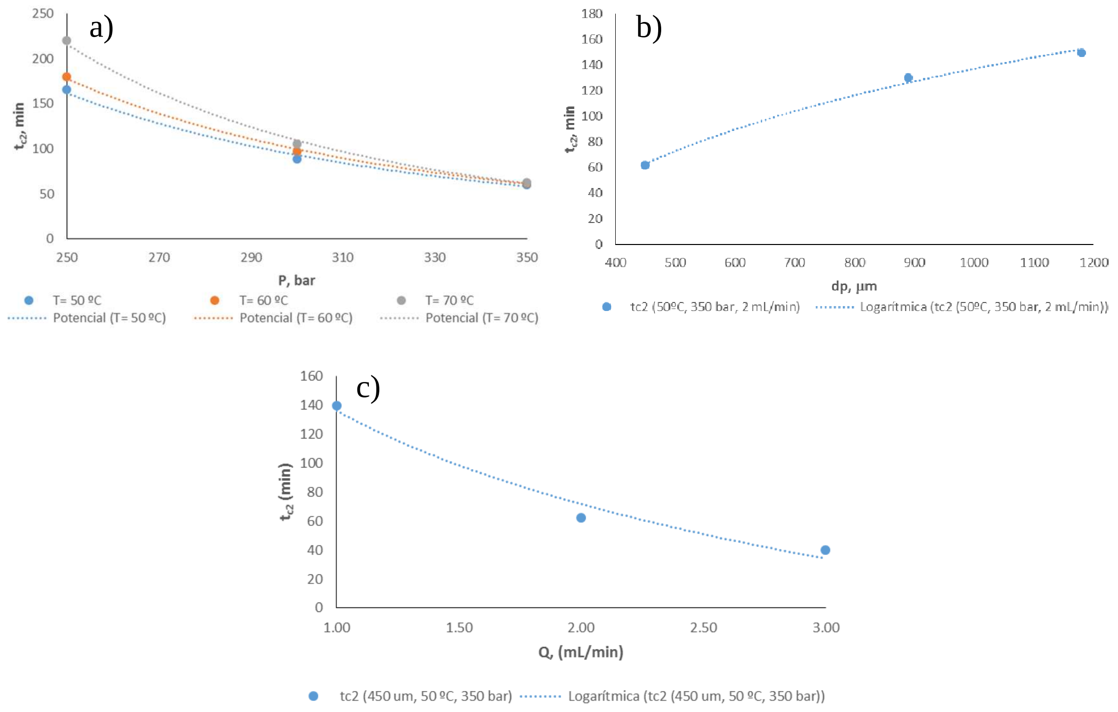

Figure 9: Breaking time evolution with temperature and pressure (a), particle diameter (b) and volumetric flow (c).

Table 7: Breaking times (t_{c1} and t_{c2}) adjustment.

t_{c2} (min)			
P(bar)	T(ºC)		
	50	60	70
300	89	97	105
250	166	180	220
350	60	62	63
R^2	0.93	0.95	0.93
t_{c2} (min)		t_{c2} (min)	
dp(µm)		Q(mL/min)	
450	62	1.00	140
890	130	2.00	62
1180	150	3.00	40
R^2	0.995	R^2	0.97
t_{c1} (min)			
P(bar)			
300	30		
250	36		

4.4. Simulation of the internal behaviour

Once the optimization has been finished, a simulation with the calculated parameters can be done. In Figure 10.b the simulation of the solid behaviour inside the column is shown. It can be checked that the calculated result agrees with the expected evolution. So, a decreasing concentration profile for each time is obtained up to reach a minimum at 90 min, when internal diffusion controls. In the same way, the liquid profile inside the column was also simulated (Figure 10.b). Obtaining, again, a decreasing concentration with time (due to solid exhaustion) up to another minimum at 90 min. These simulation would be useful to understand how the extraction process is and to estimate would the composition of the solid at any time and any point, which would be one of the main variables to decide to stop the process.

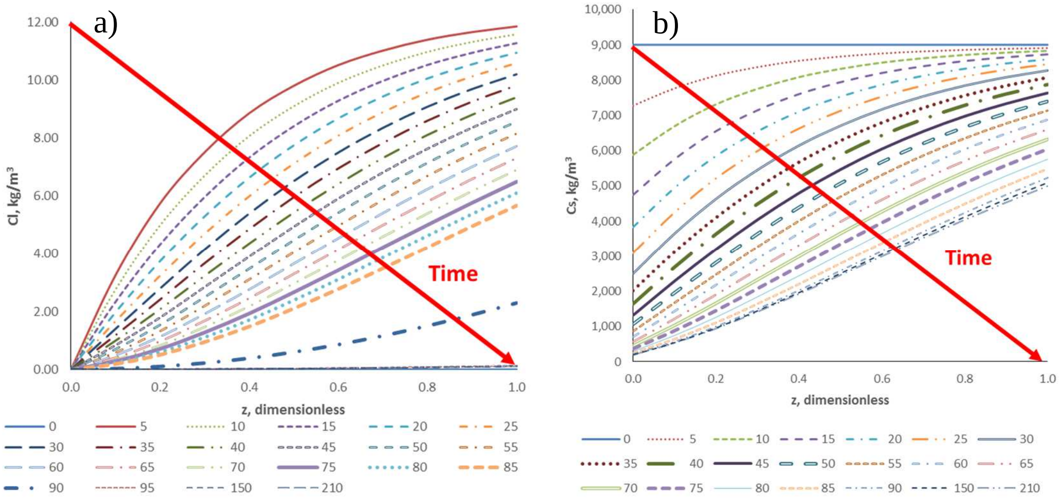

Figure 10: Internal behaviour of the liquid (a) and solid (b) simulation in experiment 1.

5. Excel interface considerations

As it was remarked in section 1, an easy-understudying Excel interface has been developed to adjust the experimental data of a SFE process. This interface also simulates the behaviour inside the column in both phases (SCF and solid), allowing to the user to analyse the effect of the operational variables. This program (for Excel 32 bytes and with a detailed manual about it) is free-available in http://hpp.uva.es/software/.

In addition, it was concluded in section 4 that this program can be used to adjust the SFE of caffeine and oil. However, it could be used with any other solid or solvent since it was based on a general model for a solid extraction processes. This last statement would be true as long as the bed porosity can be assumed as a constant and the equilibrium follows a Henry's relation. Regarding this last limitation, it can be overcome by the addition of Excel programing. So, if the user would be interested in analysing a SFE with a thermodynamic solubility calculation, they only have to include these calculations in the Excel sheet and given the solution in the Cell of the solubility. In the same way, the parameters of the thermodynamic expression can be defined as fitting parameters.

6. Conclusions

In this work the modelling for SFE processes has been assessed, developing a free available Excel interface. The model was successfully validated with two different samples, sesame seeds and coffee beans (average deviations of 7.41% and 10.35%, respectively). Moreover, the model could reproduce the effect of temperature, pressure, particle diameter and flow in all the cases and the physical sense of the fitted parameters was checked. Finally, the model was also able to simulate the behavior of the SCF and the solid inside the column, which constitutes a useful tool for understanding or teaching the process and taking operational decisions.

Acknowledgements

The authors acknowledge the Spanish Economy and Competitiveness Ministry, Project Reference: ENE2012-33613 for funding. Álvaro Cabeza would like to thank to the Spanish Ministry of Education Culture and Sports, training program of university professors (reference FPU2013/01516) for the research training contract.

Nomenclature

Acronyms

A.A.D.: Average Absolute Deviation.

SCF: supercritical fluid.

SFE: supercritical fluid extraction.

$ScCO_2$: supercritical CO_2.

BSG : brewer's spent grain.

Subindex and superindex

Y-EXP: experimental extraction yield.

Y-SIM: simulated extraction yield.

Greek letters and symbols

$\mathcal{E}$: porosity of the bed, dimensionless.

$\mathrm{C_S}$: concentration of the compound in the solid phase, kg/m^3.

$\mathrm{k_{SCF}} \cdot a_{SCF}$: external mass transfer coefficient multiplied by the specific exchange area, min^{-1}.

$\mathrm{k_S} \cdot a_S$: internal mass transfer coefficient multiplied by the specific exchange area, min^{-1}.

$K \cdot a_S$: global mass transfer coefficient multiplied by the specific exchange area, min^{-1}.

$\mathrm{C^*_{SCF}}$: equilibrium concentration in the SCF, kg/m^3.

$\mathrm{C_{SCF}}$: concentration of the in the SCF, kg/m^3.

H: equilibrium constant between the solid and the SCF, dimensionless.

F: correction factor for stage B, dimensionless.

u: SCF velocity in the column, m/min.

L: length of the column, m.

z: coordinate along the length of the reactor, dimensionless.

t: operating time, min.

t_{c_1} & t_{c_2}: breaking times, min.

$x_{i_{EXP}}$: experimental value of the fitted variable in the experiment “i”.

$x_{i_{SIM}}$: simulated value of the fitted variable in the experiment “i”.

n: total number of experiments, dimensionless.

T: operating temperature, ºC.

P: operating pressure, bar.

Q: volumetric flow, mL/min.

d_P: particle diameter, μm.

References

[1] G. Manivannan, S.P. Sawan, 1 - The Supercritical State, in: J.M.P. Sawan (Ed.) Supercritical Fluid Cleaning, William Andrew Publishing, Westwood, NJ, 1998, pp. 1-21.
[2] L. Nahar, S. Sarker, Supercritical Fluid Extraction in Natural Products Analyses, in: S.D. Sarker, L. Nahar (Eds.) Natural Products Isolation, Humana Press, 2012, pp. 43-74.
[3] E.J. Henley, J.D. Seader, Equilibrium-Stage Separation Operations in Chemical Engineering, John Wiley & Sons, Inc, 1981.
[4] S. Spinelli, A. Conte, L. Lecce, L. Padalino, M.A. Del Nobile, Supercritical carbon dioxide extraction of brewer's spent grain, The Journal of Supercritical Fluids, 107 (2016) 69-74.
[5] A. Rai, B. Mohanty, R. Bhargava, Supercritical extraction of sunflower oil: A central composite design for extraction variables, Food Chemistry, 192 (2016) 647-659.
[6] H. Nerome, M. Ito, S. Machmudah, Wahyudiono, H. Kanda, M. Goto, Extraction of phytochemicals from saffron by supercritical carbon dioxide with water and methanol as entrainer, The Journal of Supercritical Fluids.
[7] M.M.R. de Melo, A.J.D. Silvestre, C.M. Silva, Supercritical fluid extraction of vegetable matrices: Applications, trends and future perspectives of a convincing green technology, The Journal of Supercritical Fluids, 92 (2014) 115-176.
[8] E. Lack, H. Seidlitz, Commercial scale decaffeination of coffee and tea using supercritical CO2, in: M.B. King, T.R. Bott (Eds.) Extraction of Natural Products Using Near-Critical Solvents, Springer Netherlands, 1993, pp. 101-139.
[9] H. Sovová, Rate of the vegetable oil extraction with supercritical CO2—I. Modelling of extraction curves, Chemical Engineering Science, 49 (1994) 409-414.
[10] O. Döker, U. Salgin, N. Yildiz, M. Aydoğmuş, A. Çalimli, Extraction of sesame seed oil using supercritical CO2 and mathematical modeling, Journal of Food Engineering, 97 (2010) 360-366.
[11] B. Honarvar, S.A. Sajadian, M. Khorram, A. Samimi, Mathematical modeling of supercritical fluid extraction of oil from canola and sesame seeds, Brazilian Journal of Chemical Engineering, 30 (2013) 159-166.
[12] H. Peker, Srinivasan, M. P., Smith, J. M. and McCoy, B. J., Caffeine extraction rates from coffee beans with supercritical carbon dioxide, AIChE J, 38 (1992) 761–770.

[13] P. Kritzer, N. Boukis, E. Dinjus, Factors controlling corrosion in high-temperature aqueous solutions: a contribution to the dissociation and solubility data influencing corrosion processes, The Journal of Supercritical Fluids, 15 (1999) 205-227.
[14] J.M. Dobbs, J.M. Wong, K.P. Johnston, Nonpolar co-solvents for solubility enhancement in supercritical fluid carbon dioxide, Journal of Chemical & Engineering Data, 31 (1986) 303-308.
[15] Pravin Vasantrao Gadkari, Manohar Balaraman, Solubility of caffeine from green tea in supercritical CO2: a theoretical and empirical approach, Journal of Food Science and Technology, 52 (2015) 8004-8013.
[16] W. Press, S. Teukolsky, W. Vetterling, B. Flannery, Numerical recipes 3rd edition: The art of scientific computing, (2007).